lajss.org
Latin American Journal of Solids and Structures
www.lajss.org

Modular Symmetric Plate-Based Tuned Mass Damper for Scalable Multi-Frequency Vibration Suppression

Ardi Noerpamoengkas[a] 0000-0001-5666-4584, Wiwiek Hendrowati[a] 0000-0002-6034-6818, Harus Laksana Guntur[a*] 0000-0002-4998-2979

[a] Department of Mechanical Engineering, Institut Teknologi Sepuluh Nopember, Surabaya, Indonesia. Email: ardi.mech.eng@gmail.com, w_hendrowati@its.ac.id, haruslg@me.its.ac.id

* Corresponding author

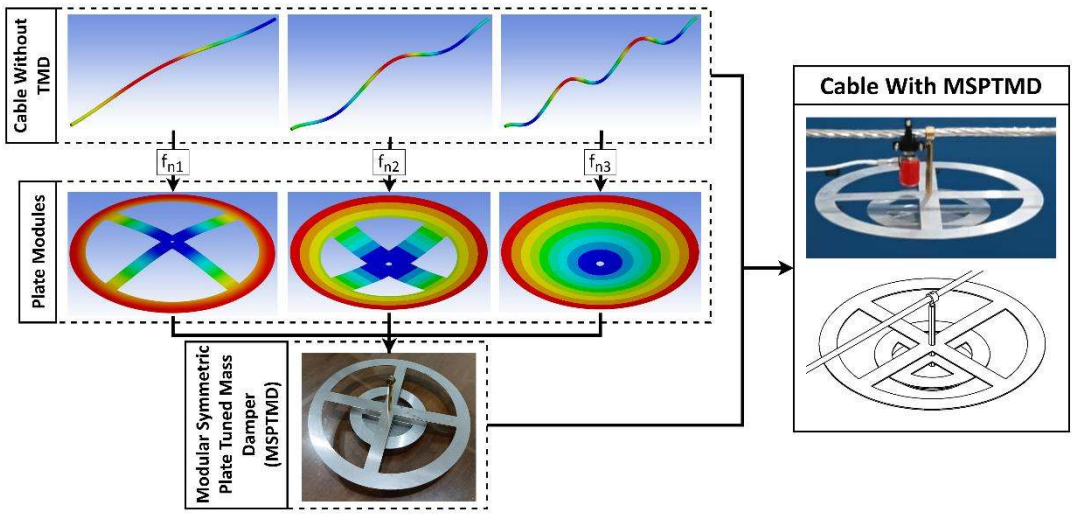
Abstract

Increasing the number of Tuned Mass Damper (TMD) natural frequencies is important for developing TMD models that cover a wider frequency range in multimodal systems. Previous research used an asymmetrical model to increase the natural frequency. The larger counterweight side of this asymmetric damper model must be placed closer to the nearest cable end to achieve better performance, which limits placement flexibility. This research developed a new multi-frequency damper model with plates, Modular Symmetric Plate TMD (MSPTMD), in which adding natural frequencies with a symmetric model and the addition method with a modular design concept are easier than existing asymmetric models. Adding natural frequencies simply requires adding plate modules. Design parameter studies were conducted to determine plate dimensions with specific natural frequencies. Three Al1100 plate modules were assembled and applied to an all-aluminium alloy cable model for three target natural frequencies in this research. The study used finite element method simulation and experiments with an electrodynamic shaker. The results show that the Modular Symmetric Plate TMD (MSPTMD) is feasible and capable of reducing vibrations at all three natural frequencies. Scalable multi-frequency vibration suppression can be achieved by adding more plate modules for more target frequencies.

Keywords

Design study, modular symmetric plate, multi-frequency, natural frequency, tuned mass damper

Graphical Abstract



1 INTRODUCTION

Tuned mass dampers (TMDs) play a crucial role in mitigating unwanted vibrations in mechanical systems by introducing an auxiliary mass-spring-damper element tuned to a specific frequency of the main structure (Ormondroyd and Den Hartog 1928; Sadek et al. 1997; Cimellaro and Marasco 2018; Rahimi et al. 2020; Yang et al. 2022; Tian 2025). All structures are susceptible to excessive vibrations when resonance occurs. One example is a cable system. Vibrations in cables are often triggered by the force exerted by wind striking them. These wind-induced vibrations are known as aeolian vibrations (Vaja et al. 2018; Liu et al. 2022). Cables possess numerous natural frequencies, and resonance can happen within specific frequency ranges that cause disturbances. When resonance occurs, it can cause cable deformation and fatigue failure (Kalombo et al. 2016; Kalombo et al. 2018; Liu et al. 2022; Yang et al. 2025). Cables/beam models are used as supporting or retaining structures in bridges, including cable-stayed bridges (Sun et al. 2022), and also serve as supports for unbalanced rotating masses (Adewusi 2020; Kumar and Kumar 2023). Cables are a primary vibration system with multiple resonances, alongside cantilever bars (Bae et al. 2012), plates (Bae et al. 2018), beams (Estruzani et al. 2025), and truss structures (Rice et al. 2017).

Traditionally, TMDs consist of attached devices on a primary structure that have one degree of freedom and can reduce the amplitude of vibrations at the specific response frequency. Their ability to mitigate vibrations has led to many investigations that have proved the effectiveness of TMDs, leading to the extensive use of tuned mass dampers in a wide range of engineering applications. These applications can utilize TMDs that consist of simple single mass, or more complex configurations.

To overcome limitations of the traditional single-mass tuned mass dampers (TMDs) in dealing with multiple resonant modes, several designs have been proposed, including, among others, plate (Mahadevaswamy and Suresh 2015), shell (Aida et al. 1998), frictional mass (Wang et al. 2022), cantilever beam (Bae et al. 2012), liquid column (Mendes et al. 2023), cable (Issa and Habchi 2012), and pendulum (Dirbas et al. 2025). These designs generally consist of multiple tuned mass dampers and have demonstrated a wide range of effectiveness in controlling multiple vibration modes. Multiple tuned mass dampers work by controlling multiple vibration modes when the system components have different natural frequencies and are individually tuned to different natural frequencies of the main system. Several of these designs include dampers with adjustable parameters to address diverse vibration characteristics (Jalili and Esmailzadeh 2002; Jalili and Esmailzadeh 2003; Gao et al. 2020). However, a single simple tuned mass damper remains the most commonly implemented device for controlling multimodal or multiresonant vibration systems because of its straightforward design.

In multimodal or multiresonant systems, applying a simple single-tuned mass damper (TMD) can reduce the vibration response at a single dominant frequency. However, it performs even poorer performance when the number of resonant frequencies increases (Cheung and Wong 2009; Hao et al. 2026). Several experiments and simulations are proving that, when used, a single TMD will reduce vibrations at the frequency it was designed for. However, other vibration modes remain largely unchanged. This leads to a partial solution to the vibration problem. This is because a single TMD is designed for a single natural frequency; therefore, when the system has many resonance peaks, a single TMD is not an adequate solution. The best approach for improving vibration control systems is to develop advanced TMD systems that can deal with multiple modes.

For dealing with multimodal vibration systems, significant progress has been made by developing improved TMD systems with multiple tuned mass dampers (Elias et al. 2016; Gill et al. 2017; Stanikzai et al. 2019; Matin et al. 2020). These systems prove to be more effective for vibration control, as seen in an experimental setup with drastically reduced vibration amplitudes. The system is configured to have several auxiliary masses, each tuned to different natural frequencies, thus extending the frequency range of the vibration suppression. This system offers more control over a multi-resonant vibration system than the conventional single TMD system.

Multimodal tuned mass dampers, such as the Stockbridge damper, reflect the variant design integrated with multiple tuned mass dampers in practical engineering systems (Wagner et al. 1973; Barry et al. 2015; Malla et al. 2021; Kaviyarasu A et al. 2024). By operating over several natural frequencies, these dampers improve the dynamic stability and control the vibration responses of cable and overhead line structures. Research has confirmed that multimodal TMDs can significantly decrease the oscillation amplitudes across several modes and increase structural resilience. Multimodal TMD design addresses the behavior of complex vibrations in multimodal systems through design and tuning strategies.

The design of multimodal tuned mass dampers is based on the use of an asymmetrical configuration, which enables the selective tuning of several modes to address multiple natural frequencies of the primary vibration system (Vaja et al. 2018). The dampers reduce multiresonant vibration responses by placing components that interact with the different vibration modes of the system. The asymmetrical configuration approach allows an extensive coverage of the frequencies

and improves the attenuation of the different modes of vibration of the system. Hence, these dampers are effective solutions to complex vibration challenges that are beyond the capability of conventional symmetric single-mass dampers.

Models of asymmetric dampers have limitations, such as sensitivity to damper placement and the introduction of uneven loads, which generate extra torque and diminish overall efficacy. For optimal damper performance, damper placement should be as accurate as possible (Luo et al. 2011; Barry et al. 2012). As far as the usage of the asymmetric Stockbridge damper is concerned, the larger counterweight must be placed on the side closest to the end. Research shows that counterweight placement is critical for effective damping, and poor placement may cause structural problems. Therefore, there is a need to design multimodal tuned mass dampers with symmetrical configurations that can achieve an overall balanced load and effectively target multiple natural frequencies. Among possible symmetrical designs, plate-based TMDs offer a potentially stable and high-performing option.

Tuned mass dampers employing plate (Snowdon 1975; Kerlin 1988; Hsu et al. 2013) or cantilever rod (Jalili and Esmailzadeh 2002; Jalili and Esmailzadeh 2003; Bae et al. 2018; Yin et al. 2021; Rezaei et al. 2023) models with additional mass have demonstrated effective vibration reduction in multimodal or multiresonant systems. These dampers use the cantilever plate or rod as a spring element, providing stiffness that interacts with the added mass to create a tuned system. This configuration enables precise tuning to specific vibration modes, with the additional mass increasing inertia and enhancing vibration counteraction. The design flexibility of these models allows customization for various structural requirements, underscoring their importance in advanced vibration mitigation strategies.

On the other hand, tuned mass dampers with plates (Mahadevaswamy and Suresh 2014; Mahadevaswamy and Suresh 2015) and with cantilever rods (Jacquot and Foster 1977; Ardayfio 1982; Yamaguchi and Saito 1984; Cavacece and Vita 2004) without additional mass have shown to reduce vibration response. In this configuration, the cantilever plate and rod are both the spring and mass elements of the system. The main vibration system is loaded, which increases the deflection and reduces the system's natural frequency. This improves alignment for tuning of the damper and the primary structure. This method is a compact way to design a damper because it eliminates the need for separate mass components. This reduces damper complexity and cost while still providing effective vibration mitigation.

The natural frequency of a tuned mass damper equipped with a massless cantilever plate or rod is primarily influenced by its geometric dimensions (Jacquot and Foster 1977; Ardayfio 1982). Adjusting the cantilever length and cross-section (thickness and width) changes both the cantilever stiffness and mass distribution, causing the damper's natural frequency to change. The plate can be configured in several ways (typically as a strip or a circular form), with each configuration providing its own tuning characteristics. These geometric configurations provide multiple degrees of freedom in damper design, enabling performance optimization for a given application of vibration control.

Introducing holes into the plate effectively reduces its natural frequency by altering stiffness and mass distribution (Slot and O'donnell 1971; Jeong and Jhung 2017; Barry and Tanbour 2018). Evidence shows that variations in hole size and number can significantly influence the plate's vibrational properties. This method offers a lightweight and practical approach to frequency adjustment without adding mass. The new application of plates with and without holes thus enables the design of multiple-plate TMDs with multiple natural frequencies and symmetrical configurations in this research.

Research, both past and present, on TMDs for multiresonant main systems has focused on the challenge of enhancing the TMD's natural frequency to cover a broader spectrum of main-system frequencies. The current TMD model uses an asymmetric approach by increasing the amount of TMD's stiffness and mass. Additionally, earlier studies on asymmetric TMDs have shown that positioning a larger TMD counterweight mass toward the end of the cable model improves performance, thereby limiting its placement flexibility. This research introduces a novel approach by employing a Modular Symmetric Plate Tuned Mass Damper (MSPTMD) model with a symmetrical modular configuration. This TMD model provides scientific contributions to attenuating multiresonant vibrations with a symmetrical configuration for placement flexibility and a modular configuration for ease of assembly and increasing the number of natural frequencies. Unlike previous studies, which have predominantly focused on asymmetrical or single-plate TMDs, this work explores the potential of plate TMDs that inherently possess multiple natural frequencies. The natural frequencies of these plates can be finely adjusted by modifying hole dimensions and adding more plate modules, enabling tailored tuning to the main system's natural frequencies for scalable multi-frequency vibration suppression. The main conclusion of this MSPTMD model application is reduced cable vibration response at several target natural frequencies.

2 MATERIALS AND METHODS

The flowcharts in Figure 1 and Figure 2 show the simulation and experimental study process, as well as the sequence of determining the plate design used for MSPTMD. Initial studies were conducted using simulations and experiments on

an undamped cable model. The target natural frequencies were determined. Several plates were designed to meet the target natural frequencies. The plates were assembled as an MSPTMD and attached to the cable. The cable's vibration conditions with the MSPTMD were compared to conditions without it.

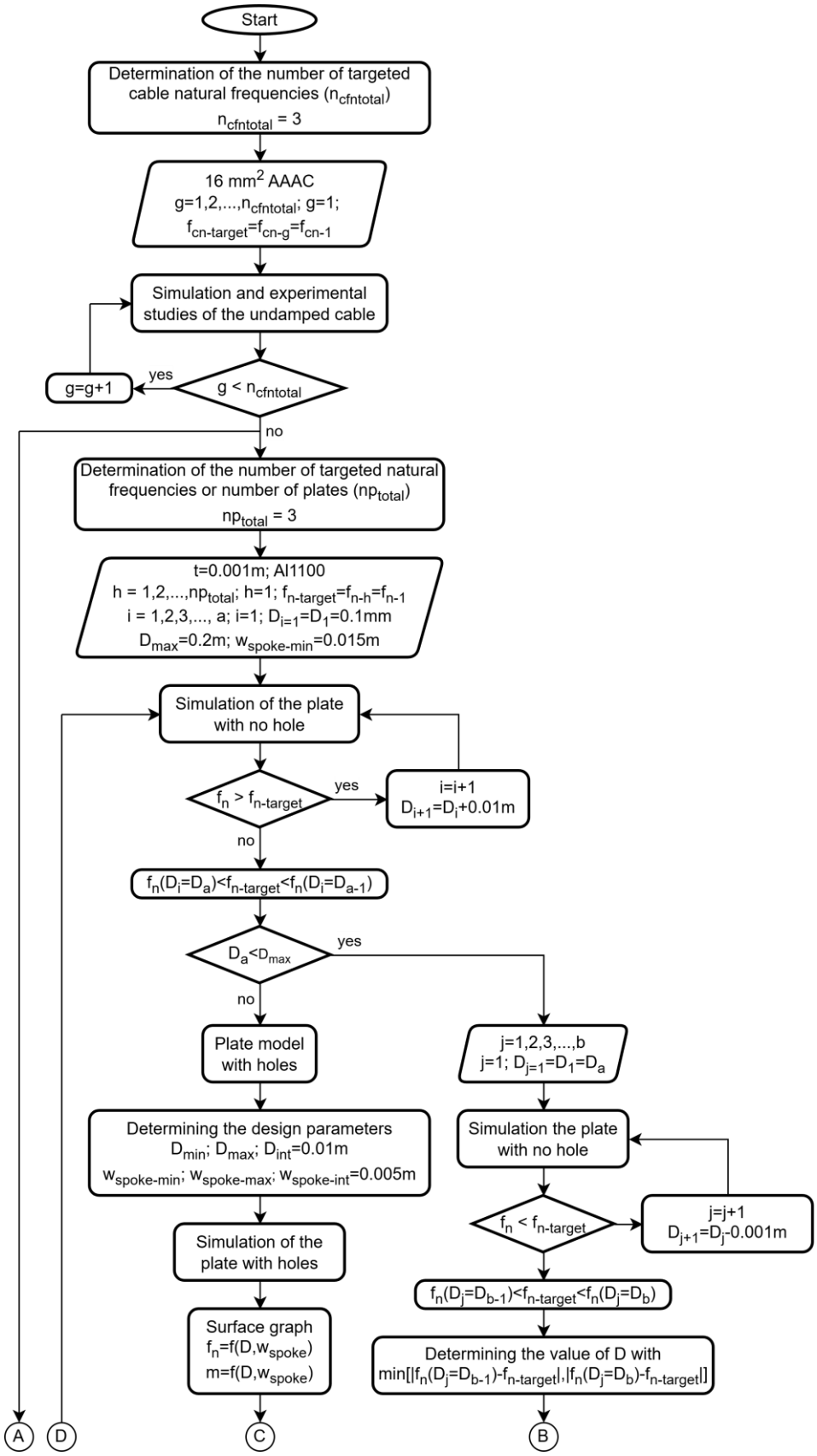


Figure 1 Flowchart of the research framework (part 1).

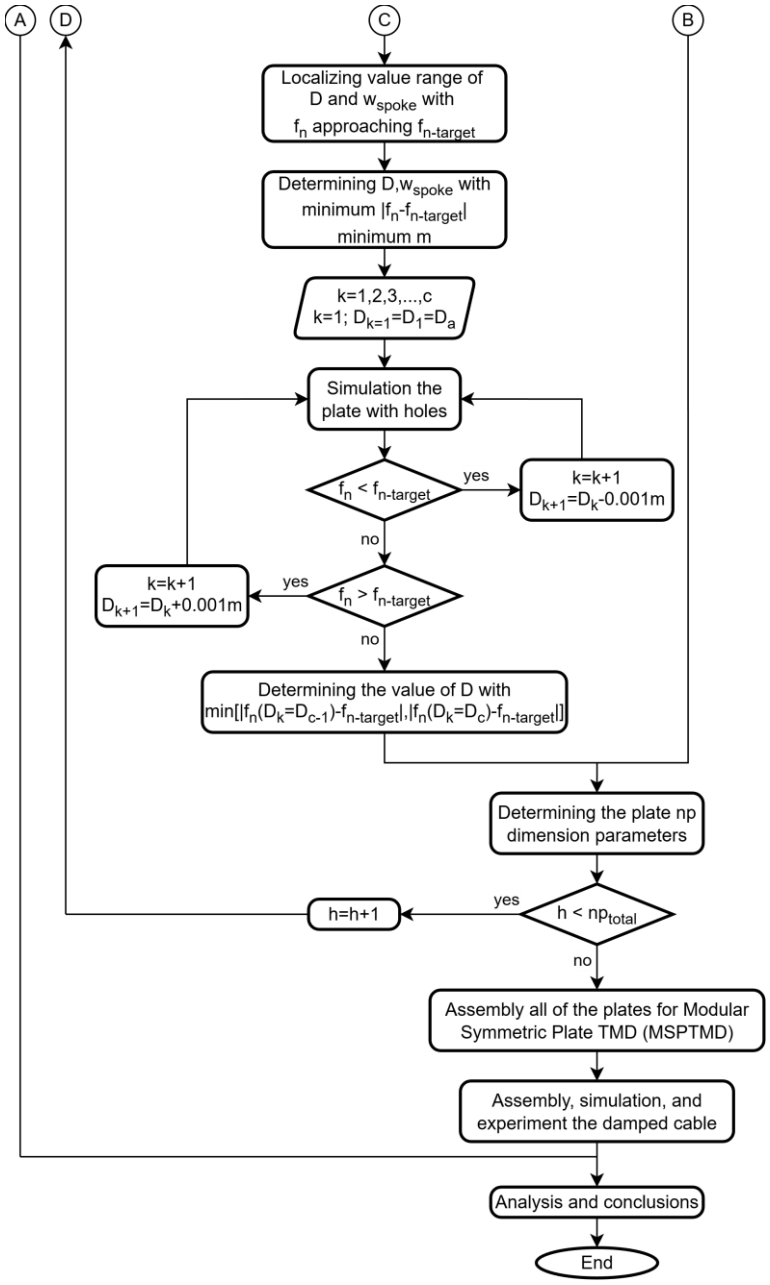


Figure 2 Flowchart of the research framework (part 2).

Table 1 Dimensions and material properties of the cable model for simulation purposes.

Parameters and properties	Value
Diameter	0.00494 m
Length	0.425 m
Density	2797 kg/m^3
Young's Modulus	2781.5 MPa
Poisson's Ratio	0.33

In this study, the cable model uses a 16 mm² All Aluminium Alloy Cable (AAAC) as the main vibration system. Because of the limited space of the lab-scale experiment, a small-diameter cable was chosen in order to measure the maximum values of the response that indicate resonance at low frequencies with the available sensors. Despite this, the cable's condition and size still represent the main vibration system and thus will allow resonance analysis. The cable's simple model will represent the vibration phenomena of multi-mode systems. The All Aluminium Alloy Cable (AAAC) was chosen to give a realistic basis for assessing the tuned mass damper (TMD), as this cable has unique mechanical properties. Using

the cable model, this research will study the damper's effectiveness at the cable's natural frequencies. The material properties will be verified using digital scale to measure the material's density accurately, and the modulus of elasticity will be determined using a Universal Testing Machine. Poisson's ratio is assumed to be 0.33 for aluminium and its alloys (Kováčik et al. 2018). Table 1 shows the dimensions and material properties of cable model.

In vibration analysis, a beam model featuring a circular cross-section and fixed ends is typically used to represent a cable. In this case, the cable is modeled as a beam with a constant circular cross-section and fixed at both ends. These boundary conditions realistically represent the cable's behavior in a structural system where the cable is fixed, and movement and rotation are prevented at the supports. The fixed-fixed beam model is typically used to represent the system dynamics, for example, the natural frequencies and mode shapes in this case.

The beam model is then subjected to a Harmonic Response analysis in ANSYS, where a gravity load is considered as a prestress load. The standard gravity of the Earth is applied in the negative Y direction on all parts of the beam model. The experimental study complements the simulation by providing empirical data of the cable's vibration. The initial, final, and interval frequencies are the same for both cases, the simulation and the experiment. The peak simulation and experimental response amplitudes refer to the undamped cable's resonance. This technique captures the beam's dynamic response to a realistic load. The objective of this simulation is to capture/compute the three natural frequencies of the beam model when configured for one, three, and five loops respectively. The model then evaluates the damped cable model. Table 2 shows the parameters of cable simulation.

Table 2 Parameters for simulating the cable model.

Parameters	Value or detail
Model	Beam
Mesh element size	1.5e-003 m
Mesh method	MultiZone
Number of nodes	31890
Element type	Hex20
Boundary condition	Fixed support; 2 end faces
Excitation	Acceleration; one fixed support; base excitation; Y component; 9.81 m/s^2
Observed response	Directional deformation; Y axis
Frequency response	At the center of the cable model; 1 node
Frequency ranges	10-50 Hz, 110-150 Hz, 300-340 Hz
Interval frequency value	5 Hz

To accurately simulate the dynamic behavior of the tuned mass damper, the plate's raw-material properties are determined using an undamped cable model. This plate, crafted from aluminium (Al1100) and measuring 1 mm thick, functions as a circular tuned mass damper without any extra mass. The material properties are defined according to Al1100 standards to ensure they accurately represent its mechanical characteristics. Table 3 shows the plate parameters.

Table 3 Dimension and material properties of the plate model for simulation purposes.

Parameters	Value or detail
Density	2661 kg/m^3
Young's Modulus	13610 MPa
Poisson's Ratio	0.33
Thickness	0.001 m

At the beginning of the study, the target natural frequencies of the cable whose vibrations will be damped were determined. This determination considered the shaker's capabilities and the position of the anti-nodes in the resonance shape mode, which are close to the accelerometer. The following approach accommodates the iterations of the study process, in order from the lowest natural frequency.

$$f_{cn-\mathrm{target}} = f_{cn-g} \quad (1)$$

$g < n_{cfntotal}$ for study iteration of the undamped cable.

Where $f_{cn\text{-}target}$ = target natural frequency of the cable (Hz)

$f_{cn\text{-}g}$ = g^{th} target natural frequency of the cable (Hz)
g = iteration g = 1,2,…,$n_{cfntotal}$
$n_{cfntotal}$ = number of targeted cable natural frequencies

Parametric design investigations systematically alter the dimensions of plates to meet desired natural frequencies while minimizing the mass of the tuned mass damper. This method allows for precise manipulation of the damper's dynamic characteristics by modifying geometric factors like plate diameter and hole dimensions. By employing iterative simulations and analyses, the parametric study discovers configurations that effectively balance vibration reduction with decreased structural load.

$$f_{n-target} = f_{n-h} \quad (2)$$

$h < np_{total}$ for study iteration of the MSPTMD plate.

Where $f_{n\text{-}target}$ = target natural frequency of the plate (Hz)
$f_{n\text{-}h}$ = h^{th} target natural frequency of the plate (Hz)
h = iteration h = 1,2,…,np_{total}
np_{total} = number of targeted plate natural frequencies

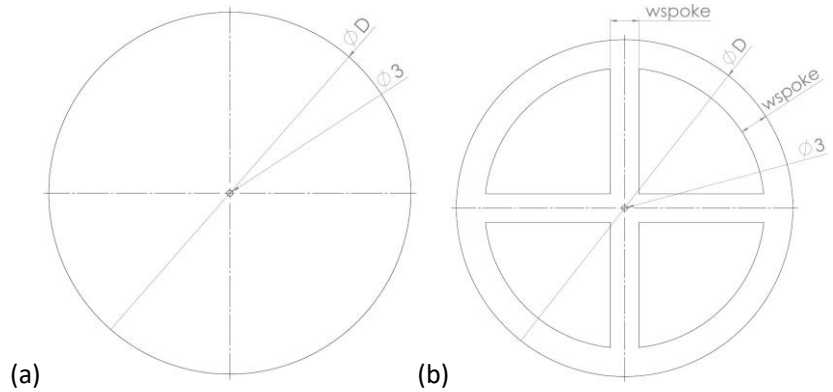


Figure 3 The illustrations depict plates without holes (a), and with holes (b).

In the parametric design study of the MSPTMD, determining the plate's outer diameter and the width of the spokes involves optimizing these dimensions to align the natural frequency as closely as possible with the target frequency while keeping the mass to a minimum. The outer diameter is determined for both models, with and without holes, whereas the spoke width is specifically calculated for the model with holes. The plate models, without and with holes, that were used in the study are shown in Figure 3. The initial phase of the parametric design study starts with the model without holes to determine the outer diameter. The simulation is repeated with progressively larger outer-diameter intervals until the natural frequency ($f_n(D_i=D_a)$) in the sequence of iterations drops below the target frequency ($f_{n\text{-}target}$).

$$f_n \ \ D_i = D_a \ \ < f_{n-target} < f_n \ \ D_i = D_{a-1} \quad (3)$$

$$D_{i+1} = D_i + 0.01m$$

Where $f_n \ \ D_i = D_a \ \ $ = plate natural frequency of final iteration i (Hz)

$f_{n-target}$ = plate natural frequency (Hz)

$f_n \ \ D_i = D_{a-1} \ \ $ = plate natural frequency of iteration i before the last iteration (Hz)

D_{i+1} = diameter for the next iteration i (m)

D_i = diameter for the current iteration i (m)

i = iteration i = 1,2,3,…,a

Continue the simulation by iterating with progressively smaller intervals of the outer diameter until the natural frequency ($f_n(D_j=D_b)$) in the sequence surpasses the target natural frequency.

$$f_n \ \ D_j = D_{b-1} \ \ < f_{n-target} < f_n \ \ D_j = D_b \quad (4)$$

$$D_{j+1} = D_j - 0.001m$$

Where $f_n \ \ D_j = D_{b-1} \ \ $ = plate natural frequency of iteration j before the last iteration (Hz)

$f_n \quad D_j = D_b$ = plate natural frequency of final iteration j (Hz)

D_{j+1} = diameter for the next iteration j (m)

D_j = diameter for the current iteration j (m)

j = iteration j = 1,2,3,…,b

The outer diameter (D) is determined by identifying the smallest discrepancy between the natural frequencies from the two most recent iterations and the target natural frequency.

$$D\left\{\min\left[\begin{array}{c}\left|f_n \quad D_j = D_{b-1} \quad - f_{n-target}\right| \\ \left|f_n \quad D_j = D_b \quad - f_{n-target}\right|\end{array}\right]\right\} \tag{5}$$

Where D = outer diameter of the plate (m)

If the outer diameter surpasses the specified maximum allowable dimension, the study advances by employing the model with holes, wherein both the outer diameter and the spoke width are adjusted. The selection of the outer diameter and spoke width is based on achieving the minimal discrepancy between the natural frequency (f_n) and the target natural frequency ($f_{n\text{-target}}$), as well as attaining the lowest possible mass value (m).

$$D, w_{spoke}\left\{\begin{array}{c}\min \left|f_n - f_{n-target}\right| \\ \min \quad m\end{array}\right\} \tag{6}$$

Where w_{spoke} = spoke width of the plate (m)

f_n = natural frequency (Hz)

The spoke width is determined by the minimum value. The outer diameter is established based on the same principle as previously applied.

$$D\left\{\min\left[\begin{array}{c}\left|f_n \quad D_k = D_{c-1} \quad - f_{n-target}\right| \\ \left|f_n \quad D_k = D_c \quad - f_{n-target}\right|\end{array}\right]\right\} \tag{7}$$

$D_{k+1} = D_k + 0.001m$ if $f_n > f_{n-target}$

$D_{k+1} = D_k - 0.001m$ if $f_n < f_{n-target}$

Where $f_n \quad D_k = D_{c-1}$ = plate natural frequency of iteration k before the last iteration (Hz)

$f_n \quad D_k = D_c$ = plate natural frequency of final iteration k (Hz)

D_{k+1} = diameter for the next iteration k (m)

D_k = diameter for the current iteration k (m)

k = iteration k = 1,2,3,…,c

The parametric design study of the plate was simulated in ANSYS using the Modal analysis system and incorporating gravity load as a prestress condition. The simulation results include the plate's natural frequency and total deformation. The natural frequency is determined from the total deformation or the mode shape corresponding to vertical vibration, ensuring its relevance to the vibration-attenuation objectives. This mode-shape concept has been used in previous research to ascertain the target natural frequency of the cable model. The selection of this mode shape is crucial for tuning the plate to interact effectively with the cable's vibration characteristics, as illustrated in Figure 4. Table 4 shows the parameters of plate simulation.

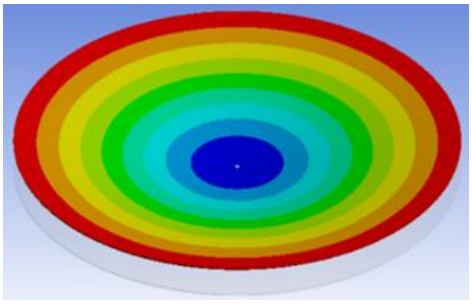
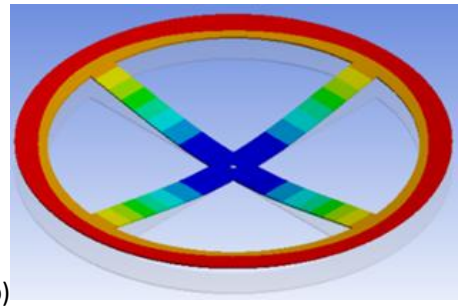
(a)  (b) 

Figure 4 The typical mode shapes of the plate without holes (a), and with holes (b) that are associated with vertical vibration.

Table 4 Parameters for simulating the plate model.

Parameters	Value or detail
Mesh method	Tetrahedrons
Mesh element size	1e-003 m
Element type	Tri3
Boundary condition	Fixed support; face of inner circle circumference

In the parametric design study, the plate's outer diameter and the spoke width were determined. The design of the model is comprehensively detailed in a drawing, which is subsequently fabricated for experimental purposes. Additionally, the 3D model is integrated with a beam-like cable model for finite element method (FEM) simulation.

The finite element method (FEM) analysis of the cable model, with and without the MSPTMD, is carried out in ANSYS using Harmonic Response analysis. Model parameters of the cable, dimensions of the MSPTMD plate, and the remaining parameters of the analysis are taken from the results of the parametric design studies. The cable-MSPTMD connector design is modeled as brass, having a Young's Modulus of 1×10^{11} Pa and a Poisson's Ratio of 0.33. All connections are bonded. The simulation primarily focuses on the cable's frequency response. It measures directional acceleration along the Y-axis at a specific node in the mesh of the cable model, which is the central node of the cable. The frequency ranges of 10-50 Hz, 110-150 Hz, and 300-340 Hz are observed, as they relate to vibration behavior and can help assess the MSPTMD's efficiency in minimizing vibrations.

For the experimental study on cable vibration with and without the MSPTMD, the cables and MSPTMD types, sizes, and materials indicated in the parametric design study will be used (Figure 5). To simulate realistic boundary conditions, the cable system will be anchored at both ends. An Ai Si Li ES-3 model electrodynamic shaker will be used to cause excitation by base motion acceleration at one end of the cable. The excitation frequency range will be close to the cable model's natural frequency for the one-, three-, and five-loop conditions. To capture acceleration signals, an Omega ACC-103 accelerometer will be attached at the cable midpoint. The acceleration signals will be sent to a PicoScope 2000 series oscilloscope for data collection and analysis.

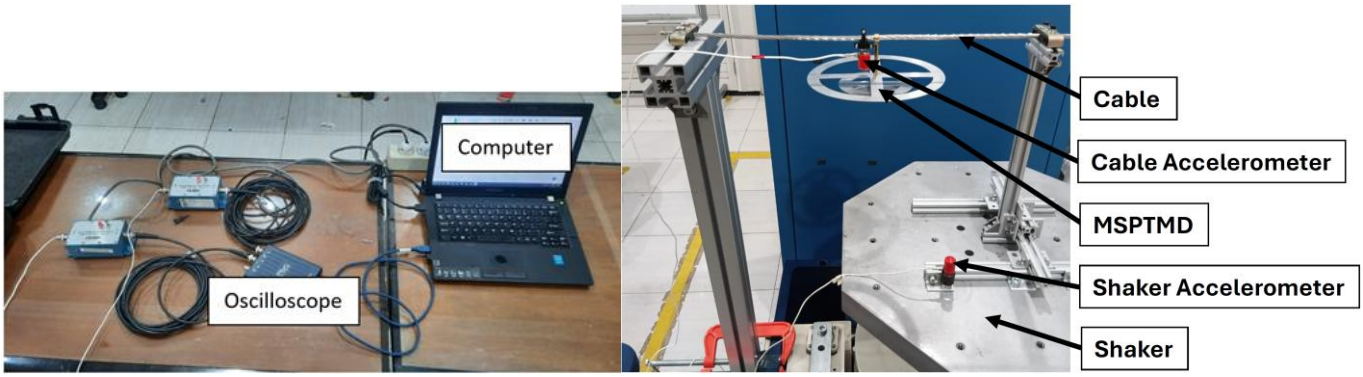


Figure 5 Experimental setup.

Acceleration response amplitudes were derived from both simulation and experimental acceleration data. The acceleration amplitude ratio is the ratio between the response and excitation acceleration amplitudes. The ratio was calculated and plotted in the frequency domain for four cases: simulation without MSPTMD, simulation with MSPTMD, experiment without MSPTMD, and experiment with MSPTMD. The comparison of the amplitude ratios for the system, both with and without the MSPTMD, was used to assess the performance of the MSPTMD with respect to the reduction of vibration.

Higher natural frequencies of the cable model were the focus of some additional simulations since the lowest natural frequency of the cable model was already validated. Additional target frequencies were created in the model, and a new MSPTMD plate was designed for each of the new natural frequencies. The new designs of the MSPTMD plate were created and adjusted parametrically to enable precise tuning, allowing the MSPTMD to effectively reduce vibration at additional frequencies of the cable model.

3 RESULTS AND DISCUSSION

3.1 Design and Simulation of MSPTMD

Simulations and experiments involving the undamped beam-like cable model identified natural frequencies of 25 Hz, 130 Hz, and 320 Hz as target frequencies for damper tuning to effectively minimize cable-model vibrations. The model exhibits one-, three-, and five-loop vibration modes, as depicted in Figure 6. These frequencies form the foundation for assessing the tuned mass damper's effectiveness in reducing resonant vibrations within the cable structure. According to Equation 1, it can be stated as follows.

$$f_{cn-1} = 25Hz$$

$$f_{cn-2} = 130Hz$$

$$f_{cn-3} = 320Hz$$

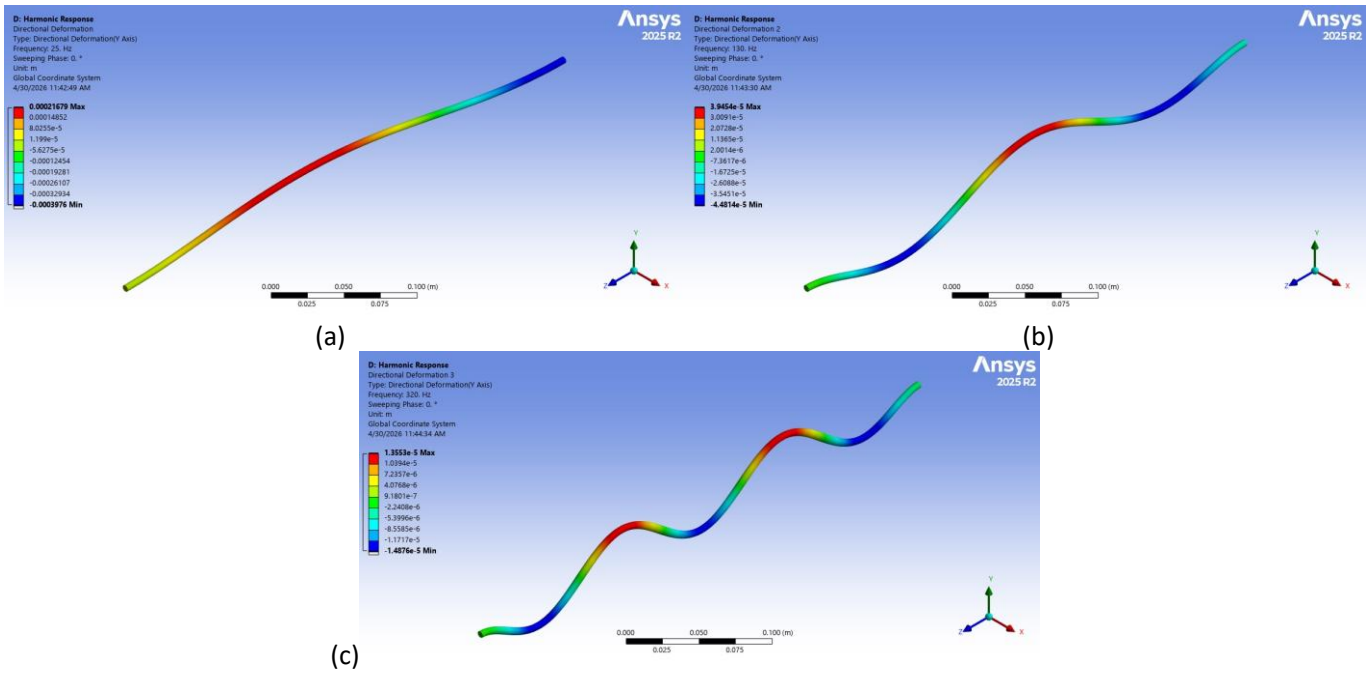


Figure 6 The mode shapes of the undamped cable model in one (a), three (b), and five (c) loop modes.

The MSPTMD plates are designed according to the target natural frequency. According to Equation 2, it can be expressed as follows.

$$f_{n-1} = 25Hz$$

$$f_{n-2} = 130Hz$$

$$f_{n-3} = 320Hz$$

The following is a parameter study result for an MSPTMD plate with a natural frequency of 25 Hz and a maximum outer diameter of 0.2 m. It is the first parametric design study without any holes. According to Equation 3, it can be expressed as follows.

$$f_n \quad D_a = 0.26m \quad < 25Hz < f_n \quad D_{a-1} = 0.25m$$

$$24.67Hz < 25Hz < 26.69Hz$$

Since the range of plate diameter sizes for a natural frequency of 25 Hz is greater than 0.2 m, the second parametric design study was conducted. This study used a plate model with holes and varied spoke width sizes. The following is the study result.

$$f_n \quad D = 0.19m, w_{spoke} = 0.015m \quad = 25.68Hz$$

$$\left| f_n - f_{n-target} \right| = \left| 25.68Hz - 25Hz \right| = 0.68Hz$$

$$f_n \quad D = 0.20m, w_{spoke} = 0.015m \quad = 22.85Hz$$

$$\left|f_n - f_{n-target}\right| = \left|22.85Hz - 25Hz\right| = 2.15Hz$$

$$f_n \quad D = 0.20m, w_{spoke} = 0.025m \quad = 27.36Hz$$

$$\left|f_n - f_{n-target}\right| = \left|27.36Hz - 25Hz\right| = 2.36Hz$$

$$f_n \quad D = 0.21m, w_{spoke} = 0.025m \quad = 24.27Hz$$

$$\left|f_n - f_{n-target}\right| = \left|24.27Hz - 25Hz\right| = 0.73Hz$$

$$m \quad D = 0.19m, w_{spoke} = 0.015m \quad = 0.0341kg$$

$$m \quad D = 0.20m, w_{spoke} = 0.015m \quad = 0.0361kg$$

$$m \quad D = 0.20m, w_{spoke} = 0.025m \quad = 0.0548kg$$

$$m \quad D = 0.21m, w_{spoke} = 0.025m \quad = 0.0582kg$$

According to Equation 6, it can be expressed as follows.

$$D, w_{spoke} \begin{Bmatrix} 25.68Hz \\ 0.0341kg \end{Bmatrix} = 0.19m, 0.015m$$

$$D, w_{spoke} \begin{Bmatrix} 22.85Hz \\ 0.0361kg \end{Bmatrix} = 0.20m, 0.015m$$

The next study was to obtain outer diameter values close to 25 Hz between 0.19 m and 0.20 m at intervals of 0.001 m. The following is the study result.

$$f_n \quad D_{c-1} = 0.192m \quad = 25.0711Hz$$

$$\left|f_n \quad D_{c-1} \quad - f_{n-target}\right| = \left|25.0711Hz - 25Hz\right| = 0.0711Hz$$

$$f_n \quad D_c = 0.193m \quad = 24.7747Hz$$

$$\left|f_n \quad D_c \quad - f_{n-target}\right| = \left|24.7747Hz - 25Hz\right| = 0.2253Hz$$

According to Equation 7, it can be stated as follows.

$$D\left\{\min\begin{bmatrix}\left|25.0711Hz - 25Hz\right| \\ \left|24.7747Hz - 25Hz\right|\end{bmatrix}\right\} = D\left\{\min\begin{bmatrix}0.0711Hz \\ 0.2253Hz\end{bmatrix}\right\} = D \quad 0.0711Hz \quad = 0.192m$$

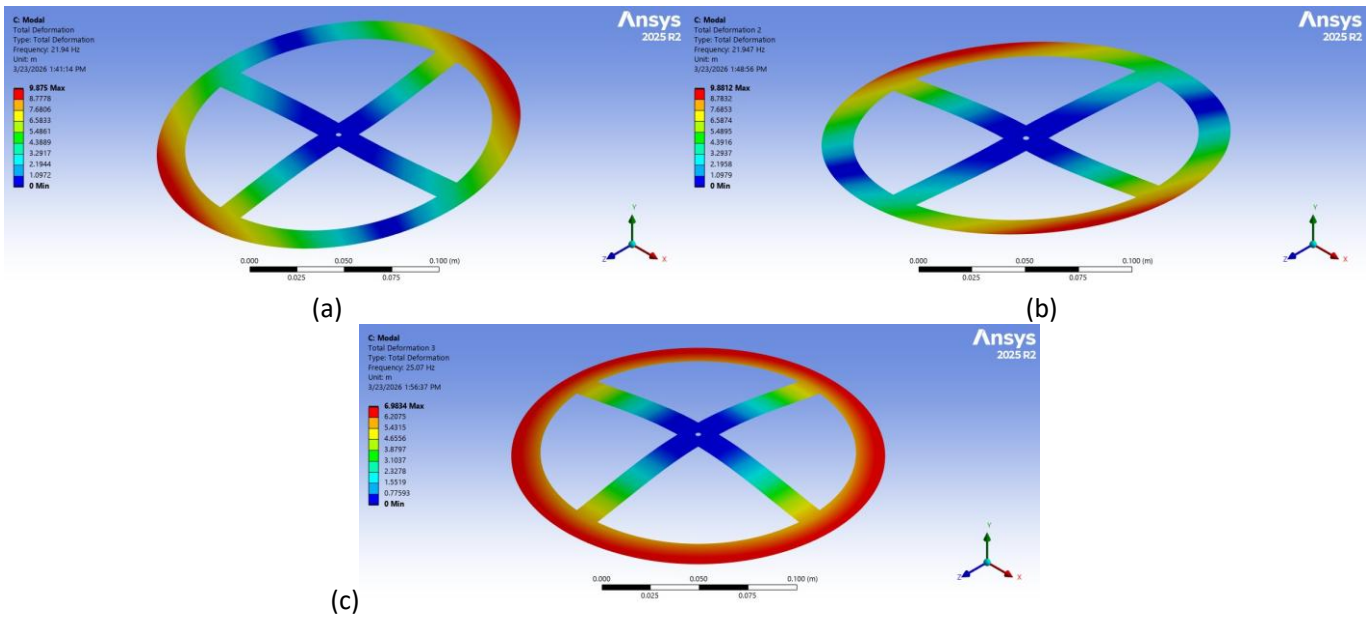
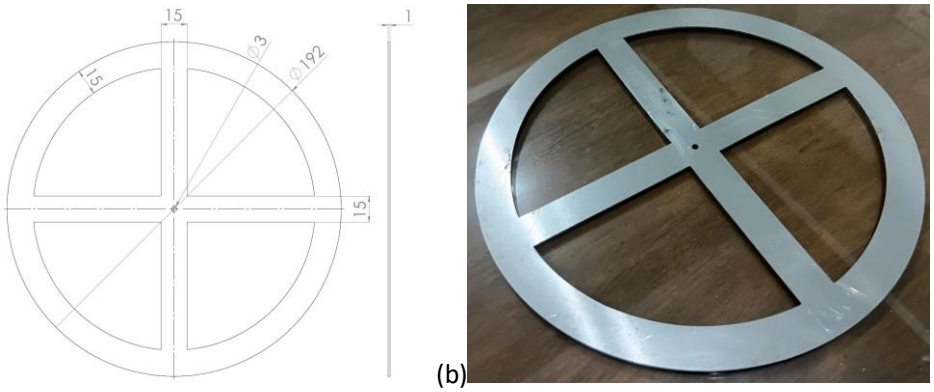


Figure 7 1st (a), 2nd (b), and 3rd (c) mode shapes of 25 Hz MSPTMD plate.

The selected outer diameter of the 1st plate was 0.192 m. The spoke width was 0.015 m. The mass is 3.449 x 10^{-2} kg. Figure 7 illustrates the initial three mode shapes of the plate. The third mode shape is chosen based on the typical

vibration mode previously mentioned. The plate dimensions with the natural frequency and mass results for the target natural frequency of 25 Hz can be seen in Table 5. Figure 8(a) presents the final detailed drawing, while Figure 8(b) displays the fabrication outcome.



(a) (b)

Figure 8 Drawing (a) and fabrication outcome (b) of 25 Hz MSPTMD plate.

Table 5 Parametric design study for the target natural frequency of 25 Hz.

D (m)	w_{spoke} (m)	f_n (Hz)	$\left\|f_n - f_{n-target}\right\|$ (Hz)	m (kg)	Selection
0.019	0.015	25.68	0.68	0.0341	No
0.0192	0.015	25.07	0.07	0.0345	Yes
0.0193	0.015	24.77	0.23	0.0347	No
0.020	0.015	22.85	2.15	0.0361	No
0.020	0.025	27.36	2.36	0.0548	No
0.021	0.025	24.27	0.73	0.0582	No

The following is a parameter study result for an MSPTMD plate with a natural frequency of 130 Hz and a maximum outer diameter of 0.1 m. It is the first parametric design study without any holes. According to Equation 3, it can be expressed as follows.

$$f_n \;\; D_a = 0.12m \;\; < 130Hz < f_n \;\; D_{a-1} = 0.11m$$

$$117.06Hz < 30Hz < 139.61Hz$$

Since the range of plate diameter sizes for a natural frequency of 130 Hz is greater than 0.1 m, the second parametric design study was conducted. This study used a plate model with holes and varied spoke width sizes. The following is the study result.

$$f_n \;\; D = 0.09m, w_{spoke} = 0.015m \;\; = 158.5Hz$$

$$\left|f_n - f_{n-target}\right| = \left|158.5Hz - 130Hz\right| = 28.5Hz$$

$$f_n \;\; D = 0.1m, w_{spoke} = 0.015m \;\; = 120.7Hz$$

$$\left|f_n - f_{n-target}\right| = \left|120.7Hz - 130Hz\right| = 9.3Hz$$

$$f_n \;\; D = 0.1m, w_{spoke} = 0.025m \;\; = 162.3815Hz$$

$$\left|f_n - f_{n-target}\right| = \left|162.3815Hz - 130Hz\right| = 32.3815Hz$$

$$f_n \;\; D = 0.11m, w_{spoke} = 0.025m \;\; = 127.4208Hz$$

$$\left|f_n - f_{n-target}\right| = \left|127.4208Hz - 130Hz\right| = 2.5792Hz$$

$$m \;\; D = 0.09m, w_{spoke} = 0.015m \;\; = 0.01353kg$$

$$m \;\; D = 0.10m, w_{spoke} = 0.015m \;\; = 0.01559kg$$

$$m \;\; D = 0.10m, w_{spoke} = 0.025m \;\; = 0.02036kg$$

$$m \;\; D = 0.11m, w_{spoke} = 0.025m \;\; = 0.02383kg$$

According to Equation 6, it can be expressed as follows.

$$D, w_{spoke} \begin{Bmatrix} 28.5Hz \\ 0.01353kg \end{Bmatrix} = 0.09m, 0.015m$$

$$D, w_{spoke} \begin{Bmatrix} 9.3Hz \\ 0.01559kg \end{Bmatrix} = 0.10m, 0.015m$$

The next study was to obtain outer diameter values close to 130 Hz between 0.09 m and 0.10 m at intervals of 0.001 m. The following is the study result.

$$f_n \quad D_{c-1} = 0.097m \quad = 130.49Hz$$

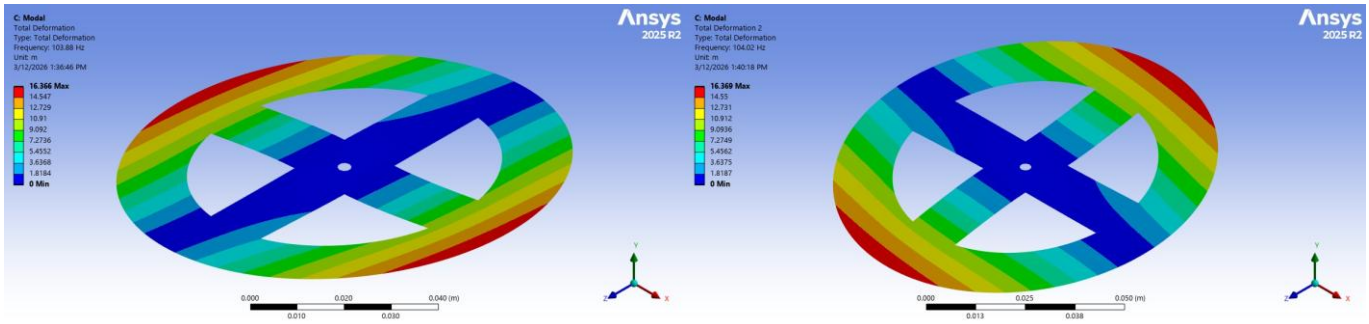
$$\left| f_n \quad D_{c-1} \quad - f_{n-\mathrm{target}} \right| = \left| 130.49Hz - 130Hz \right| = 0.49Hz$$

$$f_n \quad D_c = 0.098m \quad = 127.11Hz$$

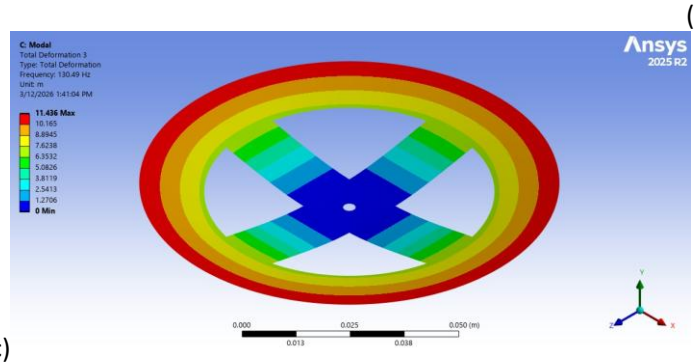
$$\left| f_n \quad D_c \quad - f_{n-\mathrm{target}} \right| = \left| 127.11Hz - 130Hz \right| = 2.89Hz$$

According to Equation 7, it can be stated as follows.

$$D\left\{ \min \begin{bmatrix} \left| 130.49Hz - 130Hz \right| \\ \left| 127.11Hz - 130Hz \right| \end{bmatrix} \right\} = D\left\{ \min \begin{bmatrix} 0.49Hz \\ 2.89Hz \end{bmatrix} \right\} = D \quad 0.49Hz \quad = 0.097m$$

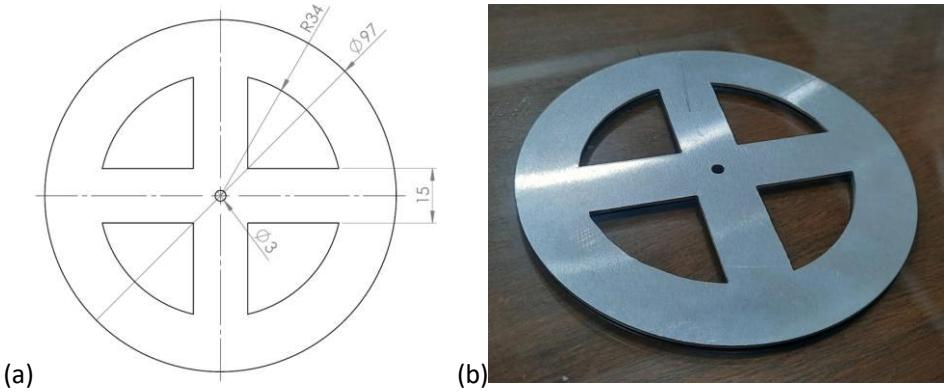


(a) (b)



(c)

Figure 9 1st (a), 2nd (b), and 3rd (c) mode shapes of 130 Hz MSPTMD plate.



(a) (b)

Figure 10 Drawing (a) and fabrication outcome (b) of 130 Hz MSPTMD plate.

Table 6 Parametric design study for the target natural frequency of 130 Hz.

D (m)	w_{spoke} (m)	f_n (Hz)	$\left\|f_n - f_{n-target}\right\|$ (Hz)	m (kg)	Selection
0.09	0.015	158.5	28.5	0.01353	No
0.097	0.015	130.5	0.5	0.01497	Yes
0.098	0.015	127.1	2.9	0.01517	No
0.10	0.015	120.7	9.3	0.01559	No
0.10	0.025	162.4	32.4	0.02036	No
0.11	0.025	127.4	2.6	0.02383	No

The selected outer diameter of the 2nd plate was 0.097 m. The spoke width was 0.015 m. The mass is 1.4969 x 10^{-2} kg. Figure 9 illustrates the initial three mode shapes of the plate. The third mode shape is chosen based on the typical vibration mode previously mentioned. The plate dimensions with the natural frequency and mass results for the target natural frequency of 130 Hz can be seen in Table 6. Figure 10(a) presents the final detailed drawing, while Figure 10(b) displays the fabrication outcome.

The following is a parameter study result for an MSPTMD plate with a natural frequency of 320 Hz and a maximum outer diameter of 0.1 m. It is the first parametric design study without any holes. According to Equation 3, it can be expressed as follows.

$$f_n \;\; D_a = 0.08m \;\; < 320Hz < f_n \;\; D_{a-1} = 0.07m$$

$$266.78Hz < 320Hz < 350.49Hz$$

The next study was to obtain outer diameter values close to 320 Hz between 0.07 m and 0.08 m at intervals of 0.001 m. The following is the study result.

$$f_n \;\; D_{b-1} = 0.073m \;\; = 321.795Hz$$

$$\left|f_n \;\; D_{b-1} \;\; - f_{n-target}\right| = \left|321.795Hz - 320Hz\right| = 1.795Hz$$

$$f_n \;\; D_b = 0.074m \;\; = 312.853Hz$$

$$\left|f_n \;\; D_b \;\; - f_{n-target}\right| = \left|312.853Hz - 320Hz\right| = 7.147Hz$$

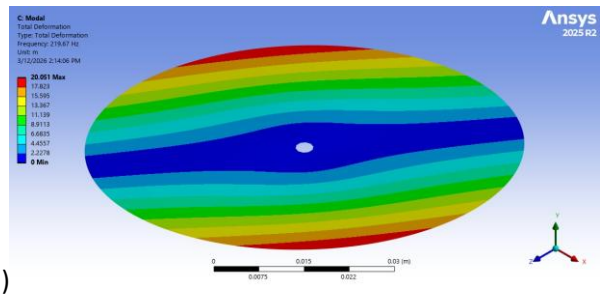
According to Equation 4, it can be expressed as follows.

$$f_n \;\; D_j = D_{b-1} = 0.073m \;\; < f_{n-target} < f_n \;\; D_j = D_b = 0.074m$$

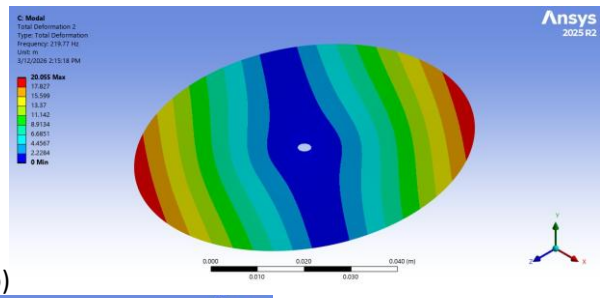
$$321.795Hz < 320Hz < 312.853Hz$$

According to Equation 5, it can be stated as follows.

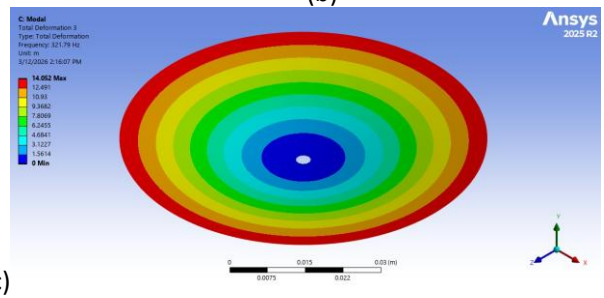
$$D\left\{\min\begin{bmatrix}\left|321.795Hz - 320Hz\right| \\ \left|312.853Hz - 320Hz\right|\end{bmatrix}\right\} = D\left\{\min\begin{bmatrix}1.795Hz \\ 7.147Hz\end{bmatrix}\right\} = D \;\; 1.795Hz \;\; = 0.073m$$



(a)

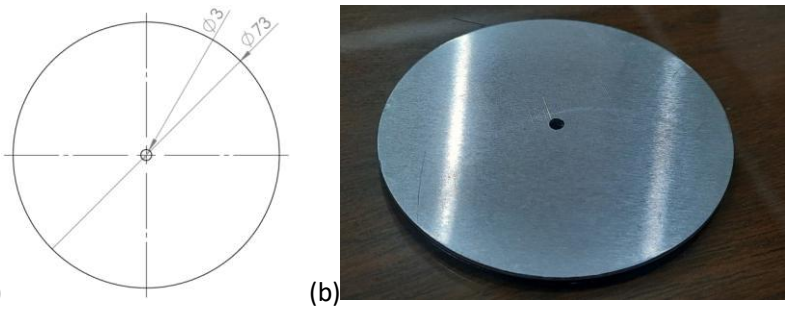


(b)



(c)

Figure 11 1st (a), 2nd (b), and 3rd (c) mode shapes of 320 Hz MSPTMD plate.



(a) (b)

Figure 12 Drawing (a) and fabrication outcome (b) of 320 Hz MSPTMD plate.

Table 7 Parametric design study for the target natural frequency of 320 Hz.

D (m)	f_n (Hz)	$\left\| f_n - f_{n-target} \right\|$ (Hz)	m (kg)	Selection
0.070	350.49	30.49	0.01022	No
0.073	321.80	1.795	0.01112	Yes
0.074	312.85	7.147	0.01143	No
0.080	266.78	53.22	0.01336	No

The selected outer diameter of the 3rd plate was 0.073 m. The mass is 1.1119 x 10^{-2} kg. Figure 11 illustrates the initial three mode shapes of the plate. The third mode shape is chosen based on the typical vibration mode previously mentioned. The plate dimensions with the natural frequency and mass results for the target natural frequency of 320 Hz can be seen in Table 7. Figure 12(a) presents the final detailed drawing, while Figure 12(b) displays the fabrication outcome.

The three plates are assembled into one unit. The combination of these plates is called an MSPTMD. All three plate modules and the cables are connected with a connector. Figure 13 shows the assembly of the MSPTMD.

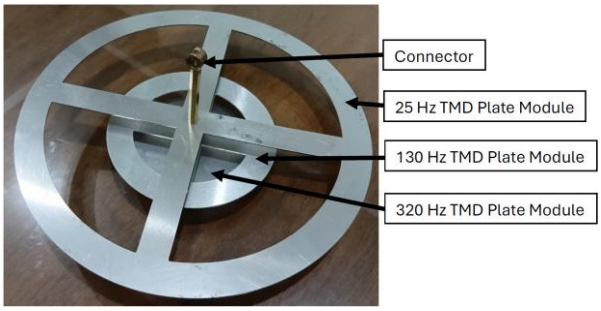


Figure 13 Assembled MSPTMD.

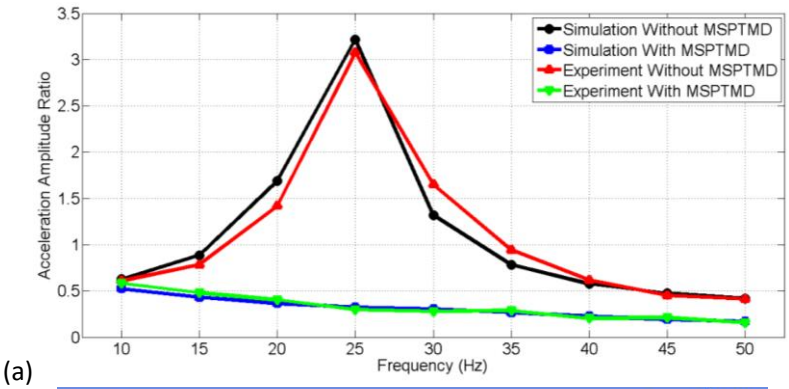
3.2 FEM Simulation and Experimental Studies

Both the FEM simulation and the experimental study highlight the MSPTMD's capability to mitigate cable vibrations effectively. In both scenarios, the amplitude ratio at the target frequency is greater when no MSPTMD is used than when the MSPTMD is applied. This decrease in acceleration amplitude verifies that the MSPTMD successfully reduces vibration in the cable model.

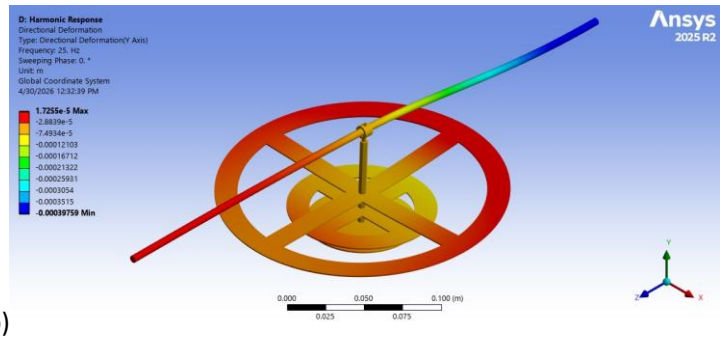
The following are the simulation and experiment results at the natural frequency of the 25 Hz cable model. Figure 14(a) shows the response reduction results. Figure 14(b) shows the active movement of the TMD plate with a natural frequency of 25 Hz in the one-loop cable vibration mode. Table 8 shows the percentage reduction in cable response due to the presence of MSPTMD.

Table 8 Comparison of amplitude ratios at the frequency of 25 Hz.

Conditions	Amplitude ratio at 25 Hz		Error (%)
	Simulation	Experiment	
Without MSPTMD	3.213	3.076	4.47
With MSPTMD	0.325	0.297	9.35
Reduction (%)	89.884	90.336	



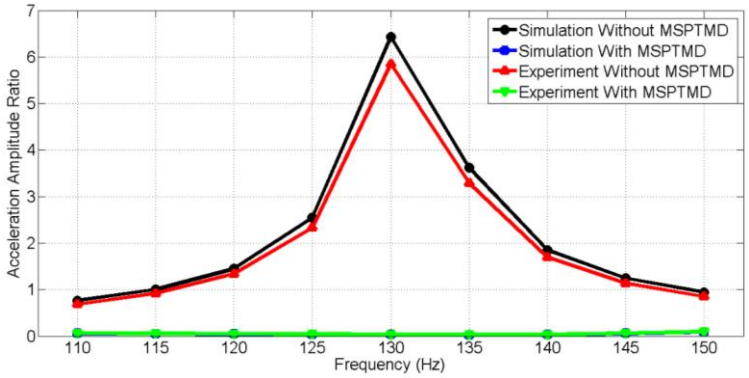
(a)



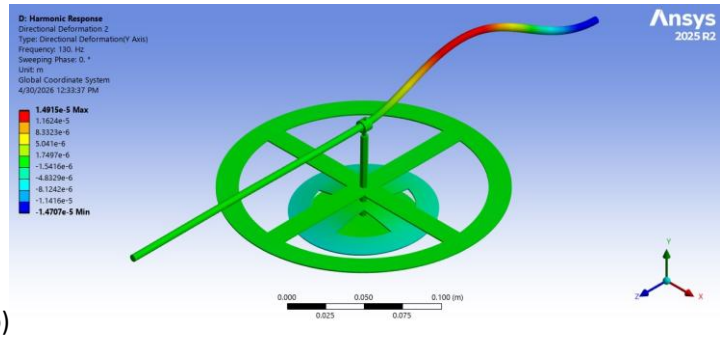
(b)

Figure 14 Results (a) for scenarios without and with the MSPTMD at frequency of 25 Hz, and the harmonic response (b).

The following are the simulation and experiment results at the natural frequency of the 130 Hz cable model. Figure 15(a) shows the response reduction results. Figure 15(b) shows the active movement of the MSPTMD plate with a natural frequency of 130 Hz in the three-loop cable vibration mode. Table 9 shows the percentage reduction in cable response due to the presence of MSPTMD.



(a)



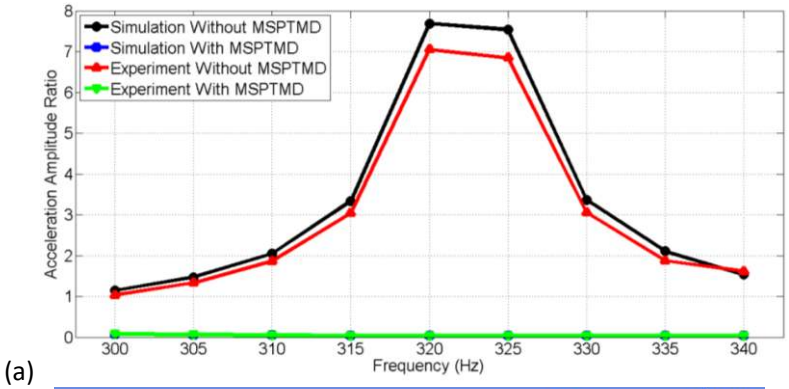
(b)

Figure 15 Results (a) for scenarios without and with the MSPTMD at frequency of 130 Hz, and the harmonic response (b).

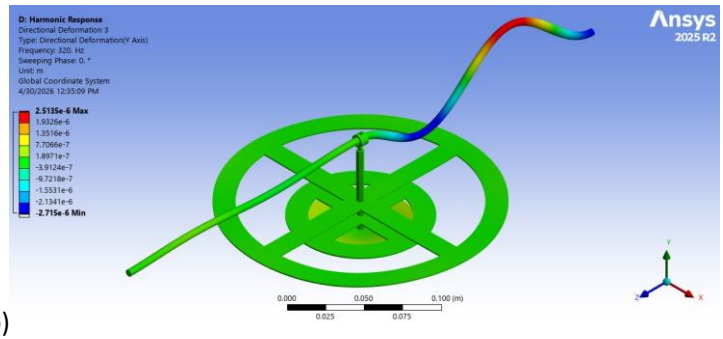
Table 9 Comparison of amplitude ratios at the frequency of 130 Hz.

Conditions	Amplitude ratio at 130 Hz		Error (%)
	Simulation	Experiment	
Without MSPTMD	6.431	5.850	9.93
With MSPTMD	0.031	0.034	9.21
Reduction (%)	99.525	99.425	

The following are the simulation and experiment results at the natural frequency of the 320 Hz cable model. Figure 16(a) shows the response reduction results. Figure 16(b) shows the active movement of the MSPTMD plate with a natural frequency of 320 Hz in the five-loop cable vibration mode. Table 10 shows the percentage reduction in cable response due to the presence of MSPTMD.



(a)



(b)

Figure 16 Results (a) for scenarios without and with the MSPTMD at frequency of 320 Hz, and the harmonic response (b).

Table 10 Comparison of amplitude ratios at the frequency of 320 Hz.

Conditions	Amplitude ratio at 320 Hz		Error (%)
	Simulation	Experiment	
Without MSPTMD	7.688	7.056	8.95
With MSPTMD	0.037	0.034	9.77
Reduction (%)	99.517	99.520	

The simulation and experimental results indicate that implementing the MSPTMD significantly mitigates the vibration response compared with a system without a TMD, as shown in Figure 14(a), Figure 15(a), Figure 16(a), Table 8, Table 9, and Table 10. Both results consistently show reduced acceleration amplitudes when the MSPTMD is utilized, thereby confirming its ability to attenuate vibrations at the targeted natural frequency. These findings are consistent with typical outcomes observed in TMD applications on primary vibration systems, thereby validating the feasibility and effectiveness of the MSPTMD design.

There are several reasons for the differences and inconsistencies between simulation and experimental values. These discrepancies may arise from simplifying the simulation model relative to the actual cable configuration, flaws in MSPTMD production, and errors in determining material properties. Nonetheless, the graphical patterns of the simulation and experimental outcomes are alike. Likewise, the natural frequency values and peak amplitude ratios from

both the simulation and experiment are similar. This suggests that the simulation is both relevant and valid when compared to the experiment.

The simulation results at the target frequency show significant deformation in both the cable and the MSPTMD plate, indicating active dynamic interaction between the two components, as shown in Figure 14(b), Figure 15(b), and Figure 16(b). This plate deformation pattern demonstrates that the MSPTMD plate is tuned to the target frequency, enabling it to absorb and mitigate vibrational energy from the cable system. This plate deformation pattern also shows conformity with the deformation pattern observed in various plate vibration modes. Only the plate vibration mode in which all sides of the plate move vertically simultaneously is used in this MSPTMD model.

Figure 14(b), Figure 15(b), and Figure 16(b) show the lowest deformation on the model side under base excitation. The cable side near the excitation experiences greater deformation than the side away from it. The maximum cable deformation with MSPTMD is lower than without it. Deformation at the MSPTMD placement point and on the cable side far from the excitation is very small.

This plate model shows its capability to minimize vibrations at a specified frequency. The model features a lightweight mass, determined during the earlier parametric design study. Moreover, the lightweight nature is achieved by removing extra masses typically used in TMD models. The plate itself is treated as an entity possessing stiffness and functioning as a mass distributed across its entire structure. This approach contrasts with other TMD models, where additional mass serves as a concentrated mass, and the stiffness component is separate. Consequently, this plate model is more straightforward compared to other TMD models.

Increasing the number of reduced target frequencies is relevant to research and development of TMD models for multiresonant vibration systems. The natural frequency target of the cable model to be damped can be increased by adding plate modules to this MSPTMD model. The addition of plate modules with assembly connectors and additional plates under the existing MSPTMD is a new design that can increase the TMD natural frequency more easily and with a symmetrical model compared to the previous asymmetrical Stockbridge damper model (Vaja et al. 2018). Vibration suppression is scalable and capable of increasing the target natural frequency by adding plate modules in the number of additional target natural frequencies. Like the previous asymmetrical Stockbridge damper model, adding target natural frequencies means adding mass and size to the TMD.

Table 11 Performance comparison of damper models.

Damper models	Reduction (%)
Traditional TMD (Zhang et al. 2023)	44.77
Tuned Mass Inerter System (TMIS) (Zhang et al. 2023)	49.25
Asymmetrical Stockbridge damper (Barry et al. 2014)	42.73
MSPTMD	89.88 - 99.52

Table 11 shows that, when assessing damper performance on the cable model, the MSPTMD is more effective at reducing performance than other damper types. The performance of traditional TMD and TMIS was measured by comparing the response amplitude to the static deformation. In contrast, the performance of the asymmetrical Stockbridge damper was characterized by the highest peak-to-peak amplitude ratio. The traditional TMD, which comprises a basic mass, spring, and damper system, and the asymmetrical Stockbridge damper, which employs varying mass sizes and messenger lengths, show relatively low amplitude reduction. This is because their damping parameters are not specifically tailored to the cable's dynamic properties. The Tuned Mass Inerter System (TMIS) shows improved performance on multi-section cables but is less efficient on single-section cables. Unlike other damper models that require extra mass, the MSPTMD operates without needing additional mass. This characteristic makes it lighter, easier to manufacture, and simpler to install, offering practical advantages alongside its vibration-damping capability. The weakness of this model is the same as other damper models, which require proper placement considerations because it cannot be moved along the cable.

Future investigations into the MSPTMD should aim to enhance its design by using optimization methods to improve its vibration-reduction capability. Although this research confirms the MSPTMD's practicality and feasibility in minimizing cable vibrations, there is still room to fine-tune its parameters for greater efficiency. Moreover, examining MSPTMD use in other primary vibration systems beyond cable structures could expand its practical applicability and flexibility. Such advancements would yield a more adaptable, optimized vibration-control solution that benefits a broader range of structural applications. Further research could also consider adding more plates. Increasing the number of plates could achieve a wider range of target natural frequencies. Moreover, additional research can be conducted on the primary

vibration system using real or industrial-scale experiments, such as testing different cable vibration systems with various sizes and types.

4 CONCLUSION

Previous and current research on TMDs for multiresonant main systems has focused on increasing the TMD's natural frequency to cover a wider range of main system frequencies. The current TMD model uses an asymmetric design by increasing the amount of TMD's stiffness and mass. Furthermore, previous research on asymmetric TMDs has shown that placing a larger TMD counterweight mass near the end of the cable model improves performance, making its placement less flexible. Main contribution of this research is a new TMD model that uses a multiresonant symmetry model concept for placement flexibility and a natural frequency addition method with a modular configuration, which is easier than the previous asymmetric damper model. The TMD model uses several circular plates assembled modularly to dampen vibrations at several target natural frequencies and is called Modular Symmetric Plate TMD (MSPTMD). The design parameter study of the plate on the outer diameter and spoke width is used to set the natural frequency. The plate model resulting from the design parameter study is used to reduce cable model vibration. The vibration study uses the finite element simulation method and experiments. The study shows that the MSPTMD is feasible and capable of reducing cable model vibrations at a few target natural frequencies. Multi-frequency vibration reduction is scalable by adding plate modules in increments of the target natural frequency. In this study, the main system consisted of an AAAC cable with target natural frequencies of 25 Hz, 130 Hz, and 320 Hz, and an MSPTMD made of 0.001 m-thick Al1100 plate. Vibration reduction ranged from 89.884% to 99.525%. The cable system's lab-scale size and small number of target natural frequencies are limitations in this research. Further research is needed to develop models using optimization methods, apply them to other main vibration systems, real or industrial-scale main systems, and add plates for more targeted natural frequencies. Further research can improve this TMD model's ability to reduce vibrations of multimodal systems.

Author's Contribuitions: Conceptualization, Ardi Noerpamoengkas, Wiwiek Hendrowati and Harus Laksana Guntur; Methodology, Ardi Noerpamoengkas, Wiwiek Hendrowati and Harus Laksana Guntur; Software, Ardi Noerpamoengkas; Validation, Ardi Noerpamoengkas; Formal analysis, Ardi Noerpamoengkas, Wiwiek Hendrowati and Harus Laksana Guntur; Investigation, Ardi Noerpamoengkas; Resources, Ardi Noerpamoengkas; Data Curation, Ardi Noerpamoengkas; Writing - original draft, Ardi Noerpamoengkas; Writing - review & editing, Wiwiek Hendrowati and Harus Laksana Guntur; Visualization, Ardi Noerpamoengkas; Funding acquisition, Ardi Noerpamoengkas; Supervision, Wiwiek Hendrowati and Harus Laksana Guntur; Project administration, Wiwiek Hendrowati and Harus Laksana Guntur.

Data Availability: Research data is only available upon request.

Editor: Marcilio Alves.

References

Adewusi S (2020) Performance of a Double-cantilever Dynamic Vibration Absorber (DCDVA) Oriented in Transverse and Longitudinal Directions. Universal Journal of Mechanical Engineering 8:265–275. https://doi.org/10.13189/UJME.2020.080504

Aida T, Aso T, Nakamoto K, Kawazoe K (1998) Vibration Control of Shallow Shell Structures Using A Shell-Type Dynamic Vibration Absorber. J Sound Vib 218:245–267. https://doi.org/10.1006/JSVI.1998.1829

Ardayfio DD (1982) Brief note: viscoelastic modelling of cantilever vibration absorbers. Mathematical Modelling 3:183–189. https://doi.org/10.1016/0270-0255(82)90023-9

Bae JS, Hwang JH, Roh JH, Kim JH, Yi MS, Lim JH (2012) Vibration suppression of a cantilever beam using magnetically tuned-mass-damper. J Sound Vib 331:5669–5684. https://doi.org/10.1016/J.JSV.2012.07.020

Bae JS, Park JS, Hwang JH, Roh JH, Pyeon B Do, Kim JH (2018) Vibration Suppression of a Cantilever Plate Using Magnetically Multimode Tuned Mass Dampers. Shock and Vibration. https://doi.org/10.1155/2018/3463528

Barry O, Oguamanam DCD, Lin DC (2012) Aeolian vibration of a single conductor with a Stockbridge damper. http://dx.doi.org/101177/0954406212452064 227:935–945. https://doi.org/10.1177/0954406212452064

Barry O, Zu JW, Oguamanam DCD (2015) Nonlinear Dynamics of Stockbridge Dampers. Journal of Dynamic Systems, Measurement and Control, Transactions of the ASME 137. https://doi.org/10.1115/1.4029526/473920

Barry O, Zu JW, Oguamanam DCD (2014) Forced vibration of overhead transmission line: Analytical and experimental investigation. Journal of Vibration and Acoustics, Transactions of the ASME 136. https://doi.org/10.1115/1.4027578/380462

Barry OR, Tanbour EY (2018) Resonant frequencies of perforated plates with rectangular slots. Proc Inst Mech Eng C J Mech Eng Sci 232:1247–1254. https://doi.org/10.1177/0954406216683974

Cavacece M, Vita L (2004) Optimal Cantilever Dynamic Vibration Absorbers by Timoshenko Beam Theory. Shock and Vibration 11:199–207. https://doi.org/10.1155/2004/710924

Cheung YL, Wong WO (2009) H∞ and H2 optimizations of a dynamic vibration absorber for suppressing vibrations in plates. J Sound Vib 320:29–42. https://doi.org/10.1016/J.JSV.2008.07.024

Cimellaro GP, Marasco S (2018) Tuned-Mass Dampers. Geotechnical, Geological and Earthquake Engineering 45:421–438. https://doi.org/10.1007/978-3-319-72541-3_18

Dirbas W, Diken H, Alnefaie K (2025) Enhancement of Wind Turbine Vibrational Behavior by using a Pendulum Tuned Mass Damper. Engineering, Technology & Applied Science Research 15:22580–22588. https://doi.org/10.48084/etasr.10589

Elias S, Matsagar V, Datta TK (2016) Effectiveness of distributed tuned mass dampers for multi-mode control of chimney under earthquakes. Eng Struct 124:1–16. https://doi.org/10.1016/J.ENGSTRUCT.2016.06.006

Estruzani AB, Kzam AKL, Villalba-Morales JD, Araujo IDG (2025) A finite element approach for modeling dynamic effects of prestressing in concrete beams. Latin American Journal of Solids and Structures 22:e8709–e8709. https://doi.org/10.1590/1679-7825/E8709

Gao H, Wang C, Huang C, Shi W, Huo L (2020) Development of a Frequency-Adjustable Tuned Mass Damper (FATMD) for Structural Vibration Control. Shock and Vibration 2020:9605028. https://doi.org/10.1155/2020/9605028

Gill D, Elias S, Steinbrecher A, Schröder C, Matsagar V (2017) Robustness of multi-mode control using tuned mass dampers for seismically excited structures. Bulletin of Earthquake Engineering 2017 15:12 15:5579–5603. https://doi.org/10.1007/S10518-017-0187-6

Hao Z, Kong X, Li W, Xu Q, Wang J (2026) An energy-saving method based on dynamic vibration absorbers for eccentrically stiffened plates under non-ideal induction motor excitation. European Journal of Mechanics - A/Solids 116:105910. https://doi.org/10.1016/J.EUROMECHSOL.2025.105910

Hsu YS, Ferguson NS, Brennan MJ (2013) The experimental performance of a nonlinear dynamic vibration absorber. Conference Proceedings of the Society for Experimental Mechanics Series 1:247–257. https://doi.org/10.1007/978-1-4614-6570-6_23

Issa JS, Habchi WF (2012) Vibration Suppression in a Cantilever Beam Using a String-Type Vibration Absorber. ASME International Mechanical Engineering Congress and Exposition, Proceedings (IMECE) 13:215–221. https://doi.org/10.1115/IMECE2010-40450

Jacquot RG, Foster JE (1977) Optimal Cantilever Dynamic Vibration Absorbers. Journal of Engineering for Industry 99:138–141. https://doi.org/10.1115/1.3439127

Jalili N, Esmailzadeh E (2002) Adaptive-passive structural vibration attenuation using distributed absorbers. Proceedings of the Institution of Mechanical Engineers, Part K: Journal of Multi-body Dynamics 216:223–235. https://doi.org/10.1177/146441930221600303

Jalili N, Esmailzadeh E (2003) A nonlinear double-winged adaptive neutralizer for optimum structural vibration suppression. Commun Nonlinear Sci Numer Simul 8:113–134. https://doi.org/10.1016/S1007-5704(02)00081-3

Jeong KH, Jhung MJ (2017) Free vibration analysis of partially perforated circular plates. Procedia Eng 199:182–187. https://doi.org/10.1016/J.PROENG.2017.09.230

Kalombo RB, Araújo JA, Ferreira JLA, da Silva CRM, Alencar R, Capra AR (2016) Assessment of the fatigue failure of an All Aluminium Alloy Cable (AAAC) for a 230 kV transmission line in the Center-West of Brazil. Eng Fail Anal 61:77–87. https://doi.org/10.1016/j.engfailanal.2015.08.043

Kalombo RB, Miranda TB, Rocha PHC, Ferreira JLA, Da Silva CRM, Araújo JA (2018) Fatigue performance of overhead conductors tested under the same value of H/w parameter. Procedia Eng 213:346–358. https://doi.org/10.1016/j.proeng.2018.02.035

Kaviyarasu A, Libanesh S, Keerthana S, Jaisheelan M, Vennila A (2024) A Review Paper on Analysis, Methods and Applications of Stock Bridge Dampers in Transmission Lines. International Journal of Research Publication and Reviews Journal 5:11665–11668. https://doi.org/10.55248/gengpi.5.0524.1416

Kerlin RL (1988) Predicted attenuation of the plate-like dynamic vibration absorber when attached to a clamped circular plate at a non-central point of excitation. Applied Acoustics 23:17–27. https://doi.org/10.1016/0003-682X(88)90078-3

Kováčik J, Marsavina L, Linul E (2018) Poisson's Ratio of Closed-Cell Aluminium Foams. Materials 2018, Vol 11, Page 1904 11:1904. https://doi.org/10.3390/MA11101904

Kumar RK, Kumar A (2023) Vibration attenuation of a beam supporting an unbalanced rotor using nonlinear energy sink. Journal of the Brazilian Society of Mechanical Sciences and Engineering 45:1–14. https://doi.org/10.1007/S40430-023-04064-6/METRICS

Liu J, Yan B, Mou Z, Gao Y, Niu G, Li X (2022) Numerical study of aeolian vibration characteristics and fatigue life estimation of transmission conductors. PLoS One 17:e0263163. https://doi.org/10.1371/journal.pone.0263163

Luo X, Zhang Y, Zheng Y (2011) Vibration Performance Analysis of FR Vibration Damper Using Finite Elements Method. Applied Mechanics and Materials 44–47:1268–1272. https://doi.org/10.4028/WWW.SCIENTIFIC.NET/AMM.44-47.1268

Mahadevaswamy P, Suresh BS (2015) Influence of Aspect Ratio of Vibratory Flap on Dynamic Response of Clamped Rectangular Plate. International Journal of Structural Stability and Dynamics 15. https://doi.org/10.1142/S0219455414500643

Mahadevaswamy P, Suresh BS (2014) Experimental Study on Effect of Vibratory Flap Position on Dynamic Response of Clamped Rectangular Plate with Cut-Out. Applied Mechanics and Materials 592–594:2036–2040. https://doi.org/10.4028/WWW.SCIENTIFIC.NET/AMM.592-594.2036

Malla AL, Gupta SK, Barry O (2021) Nonlinear Modeling and Analysis of Power Lines With Stockbridge Dampers Under Vortex-Induced Vibrations. ASME 2020 Dynamic Systems and Control Conference, DSCC 2020 2. https://doi.org/10.1115/DSCC2020-3154

Matin A, Elias S, Matsagar V (2020) Distributed multiple tuned mass dampers for seismic response control in bridges. Proceedings of the Institution of Civil Engineers - Structures and Buildings 173:217–234. https://doi.org/10.1680/jstbu.18.00067

Mendes MV, Ghedini LB, Batista RN, Pedroso LJ (2023) A study of TLCD parameters for structural vibration mitigation. Latin American Journal of Solids and Structures 20:1-17. e475. https://doi.org/10.1590/1679-78257412

Ormondroyd J, Den Hartog JP (1928) The Theory of the Dynamic Vibration Absorber. Journal of Fluids Engineering, Transactions of the ASME 49–50. https://doi.org/10.1115/1.4058553/1172255

Rahimi F, Aghayari R, Samali B (2020) Application of Tuned Mass Dampers for Structural Vibration Control: A State-of-the-art Review. Civil Engineering Journal 6:1622–1651. https://doi.org/10.28991/cej-2020-03091571

Rezaei M, Talebitooti R, Liao WH, Friswell MI (2023) Integrating PZT layer with tuned mass damper for simultaneous vibration suppression and energy harvesting considering exciter dynamics: An analytical and experimental study. J Sound Vib 546:117413. https://doi.org/10.1016/J.JSV.2022.117413

Rice JA, LaFave JM, Foutch DA, Abdullah ABM (2017) Passive Vibration Mitigation for Highway Sign Trusses Susceptible to Wind-Induced Vibrations. Journal of Performance of Constructed Facilities 31:04017091. https://doi.org/10.1061/(ASCE)CF.1943-5509.0001076

Sadek F, Mohraz B, Taylor A, Chung R (1997) A method of estimating the parameters of tuned mass dampers for seismic applications. Earthq Eng Struct Dyn 26:617–635

Slot T, O'donnell WJ (1971) Effective Elastic Constants for Thick Perforated Plates With Square and Triangular Penetration Patterns. Journal of Engineering for Industry 93:935–942. https://doi.org/10.1115/1.3428087

Snowdon JC (1975) Platelike Dynamic Vibration Absorbers. Journal of Engineering for Industry 97:88–93. https://doi.org/10.1115/1.3438595

Stanikzai MH, Elias S, Matsagar VA, Jain AK (2019) Seismic response control of base-isolated buildings using multiple tuned mass dampers. Structural Design of Tall and Special Buildings 28:e1576. https://doi.org/10.1002/tal.1576

Sun L, Chen L, Huang H (2022) Stay cable vibration mitigation: A review. Advances in Structural Engineering 25:3368–3404

Tian Q (2025) The damping of the dynamic vibration absorber. Scientific Reports 2025 15:1 15:13917-. https://doi.org/10.1038/s41598-025-98320-5

Vaja NK, Barry OR, Tanbour EY (2018) On the modeling and analysis of a vibration absorber for overhead powerlines with multiple resonant frequencies. Eng Struct 175:711–720. https://doi.org/10.1016/j.engstruct.2018.08.051

Wagner H, Ramamurti V, Sastry RVR, Hartmann K (1973) Dynamics of stockbridge dampers. J Sound Vib 30:207-IN2. https://doi.org/10.1016/S0022-460X(73)80114-2

Wang S, Yang G, Ji L, Bi C, Zheng C (2022) Multi-mode vibration attenuation of mistuned bladed disks by frictional tuned mass dampers array. J Sound Vib 536:117176. https://doi.org/10.1016/J.JSV.2022.117176

Yamaguchi H, Saito H (1984) Vibrations of beams with an absorber consisting of a viscoelastic solid and a beam. Earthq Eng Struct Dyn 12:467–479. https://doi.org/10.1002/EQE.4290120404

Yang F, Sedaghati R, Esmailzadeh E (2022) Vibration suppression of structures using tuned mass damper technology: A state-of-the-art review. JVC/Journal of Vibration and Control 28:812–836. https://doi.org/10.1177/1077546320984305/ASSET/IMAGES/LARGE/10.1177_1077546320984305-FIG15.JPEG

Yang J, Shi C, Luo Y, Yang Y, Kang H, Zhang C, Ren W, Ding B, Zheng T, Zhong Y, Liaw PK (2025) Fatigue life prediction of aluminum conductor steel reinforced under aeolian vibration based on finite element simulation. Eng Fract Mech 330:111698. https://doi.org/10.1016/J.ENGFRACMECH.2025.111698

Yin Q, Zhao J, Liu Y, Zhang Y (2021) The approximate calculation of the natural frequencies of a Stockbridge type vibration damper and analysis of natural frequencies' sensitivity to the structural parameters. Mechanical Sciences 12:863–873. https://doi.org/10.5194/MS-12-863-2021

Zhang L, Chen Q, Zhang R, Lei T (2023) Vibration control of beams under moving loads using tuned mass inerter systems. Eng Struct 275:115265. https://doi.org/10.1016/J.ENGSTRUCT.2022.115265